Journal of Physiology (1990), **431**, *pp.* 269–290
With 11 *figures*
Printed in Great Britain

M-CURRENT NOISE AND PUTATIVE M-CHANNELS IN CULTURED RAT SYMPATHETIC GANGLION CELLS

BY DAVID G. OWEN*, STEPHEN J. MARSH AND DAVID A. BROWN

From the MRC Neuropharmacology Group, Department of Pharmacology, University College London, Gower Street, London WC1E 6BT

(*Received 6 February 1990*)

SUMMARY

1. Whole-cell recordings of M-currents and single-channel recordings have been made in cultured rat sympathetic ganglion (SCG) neurones using the patch clamp technique.

2. Muscarine caused a reduction in macroscopic M-current relaxations, induced by voltage steps, and a concomitant reduction in whole-cell current noise. Power spectra of the muscarine-sensitive component of current noise were fitted with two Lorentzian components corresponding, on average, to 162 and 15 ms. The longer time constant was very similar to that of deactivation tail currents measured at the same potential.

3. The single-channel conductance at −30 mV was estimated from power density spectra and whole-cell current–variance relationships to be 1–2 pS.

4. Putative single M-channels, activated by depolarization, were identified in cell-attached and outside-out patches from cultured SCG neurones. In particular, the ensemble average of a small amplitude channel (estimated to be *ca* 4 pS in physiological $[K^+]$) in a cell-attached patch, exhibited a similar time dependence to whole-cell M-current.

INTRODUCTION

The M-current (I_M) is a time- and voltage-dependent K^+ current, originally identified in sympathetic ganglion cells (Brown & Adams, 1980; Constanti & Brown, 1981). It was called the M-current because it was inhibited by muscarinic acetylcholine-receptor agonists. However, although the kinetics of the macroscopic currents followed the usual expectations derived from the behaviour of voltage-gated ion channels (Constanti & Brown, 1981; Adams, Brown & Constanti, 1982*a*; Lancaster & Pennefather, 1987), the channels themselves have not yet been identified or characterized. Colloquially, this has been attributed to their probable low conductance, which militates against direct observations using single-channel recording techniques.

In view of this potential difficulty, we have attempted to identify and characterize the M-channels by spectral analysis of whole-cell current noise in voltage-clamped

* Present address to which reprint requests should be sent: Electrophysiology Section, Wyeth Research (UK), Huntercombe Lane South, Taplow, Berks SL6 0PH.

MS 8254

rat superior cervical ganglion (SCG) cells. We find that fluctuation analysis of the muscarine-sensitive component of membrane current in these cells indicates a single M-channel conductance of about 1–2 pS in physiological saline solution. Using this approach, Neher, Marty, Fukuda, Kubo & Numa (1988) have deduced an elementary conductance of 3 pS for the channels underlying the acetylcholine-inhibited, M-like current in transfected NG108-15 neuroblastoma hybrid cells, and some observations on bull-frog cells which are in fair accord with the present results have recently been reported in abstract form (Gruner, Marrion & Adams, 1989). We also report the presence in cell-attached membrane patches of a low-conductance single channel which might be appropriate for an M-channel. A preliminary report of some of our data has been given to the Physiological Society (Marsh & Owen, 1988).

METHODS

Tissue culture and electrophysiology

SCG neurones were obtained from adult (20–23 days postnatal; 50–70 g) rats and grown in culture according to previously published methods (Marrion, Smart & Brown, 1987). Animals were killed using nitrous oxide. After a period of 3–6 days in culture, electrophysiological recordings were made using either an Axoclamp 2A voltage clamp amplifier (Axon Instruments, Inc.) or a deVilliers patch clamp amplifier (DevTech Ltd). In either case patch electrodes were used to make recordings (Hamill, Marty, Neher, Sakmann & Sigworth, 1981). These were fire-polished, coated with Sylgard elastomer (Corning) to reduce stray capacitance, and filled with a recording solution which consisted of (mM): 150 potassium gluconate, 30 KCl, 2 $MgCl_2$, 5 HEPES, 0·5 EGTA (0·1 μM-free Ca^{2+}), and 1 ATP (after Marrion *et al.* 1987). The pipette solution was buffered to pH 6·8 in order to reduce the incidence and degree of 'wash-out' of the M-current (Brown, Marrion & Smart, 1989). In some cases 200 μM-GTP was also included in the pipette solution. Typical electrode resistances were 5–8 MΩ. The bathing solution normally consisted of (mM): 144 NaCl, 2·5 KCl, 2 $CaCl_2$, 2 $MgCl_2$, 5 HEPES, 10 glucose, pH 7·4. In some experiments using the cell-attached patch configuration, the patch pipette was filled with a high $[K^+]$ recording solution which consisted of (mM): 180 KCl, 2 $MgCl_2$, 2 $CaCl_2$, 5 HEPES, pH 7·4, and in some cases 1 μM-apamin (Serva) was also included in this solution. Inside-out patch recordings were made using the pipette-filling solution normally used in whole-cell recording and the normal bathing solution (above).

Data acquisition

Whole-cell currents were digitized and acquired on line using a PDP-11/23 computer (Digital Equipment Corporation) via a CED-502 interface (Cambridge Electronic Design) running DA8 (D.G.O.) software, a descendant of DA5 (J. C. Wise, Sandoz Institute for Medical Research). For the purposes of fluctuation analysis, whole-cell currents (both DC- and AC-coupled) were also recorded on videotape using a Sony Betamax and modified Sony PCM. This data was subsequently bandpass filtered using 8-pole Butterworth filters (Barr & Stroud), digitized via the CED-502 interface and acquired and analysed by a PDP-11/73 computer running software supplied by D. Colquhoun (University College London) and in some cases NAQ5 (J. Dempster, University of Strathclyde) running on a PDP-11/23 computer. Single-channel recordings were made using the deVilliers patch amplifier in cell-attached and outside-out patch configurations (Hamill *et al.* 1981) and data were acquired using DA8.

Current analyses

Current and voltage measurements were made using cursor-based routines in DA8. Digital subtraction of raw data records (e.g. ±muscarine) and averaging of raw records were also performed with DA8. In some cases, raw data records were edited using DA8 in order to construct baseline currents for leak subtraction purposes. This procedure enables sections of a data record to be replaced with an idealized segment derived from some other region of the record. The value of the idealized segment is obtained by averaging a user-defined number of data points around the cursor position (usually 5–10% record length). This technique was particularly useful in single-channel voltage-jump experiments where it was not always possible to obtain null current records

for leak subtraction. The method was also used in the preparation of single-channel data for construction of histograms where there might be unwanted channels contaminating the record (see Results). Individual data records could be translated to ASCII format from DA8 and thence read by a variety of general analysis software. In particular GRAPHPAD (ISI Software) was used to fit exponential functions to whole-cell tail currents and single-channel ensemble data. This program was also used to fit parabolas to current–variance plots. This program uses a non-linear least-squares procedure based upon the method of Marquardt (1963). Histograms of single-channel amplitude data were fitted with Gaussian functions using pSTAT (Axon Instruments Inc.) and plotted using GRAPHPAD.

Current fluctuation analysis

Spectral density functions ('power spectra') were estimated for whole-cell currents recorded in the presence and absence of muscarine (i.e. a proportion of I_M, activated by depolarizing the cell, was blocked). Muscarine was normally applied by diffusion from a micropipette containing a 10–50 μM solution, which was positioned in close proximity to the cell ($< 10\ \mu$m). Stretches of contiguous data were sampled such that the minimum recording time was equal to the reciprocal of the desired frequency resolution (f_{res}). In practice, control and test noise were sampled for periods of between 5 and 10 min in order to provide sufficient data to average a number of power spectra (see below). Current fluctuations were analysed as follows: one-sided spectra were obtained in the presence and absence of muscarine with a fast Fourier transform as described by Colquhoun, Dreyer & Sheridan (1979). Average spectra (obtained from fourteen to twenty-two individual 2048-point spectra; resolution 0·05 Hz) were calculated for each of the two conditions ($\pm$muscarine) and were then subtracted to give a 'net spectrum' which represented *muscarine-sensitive current*. These were then fitted with one or more (normally two) Lorentzian functions of the form:

$$G(f) = \frac{G(0)}{1+(f/f_c)^2}, \tag{1}$$

where $G(f)$ is the one-sided density at frequency f, $G(0)$ is the zero frequency asymptote and f_c is the cut-off frequency (frequency at which the spectral density falls to half of $G(0)$). Lorentzian functions were fitted to the data by the method of weighted least squares (see Colquhoun *et al.* 1979). In most cases two Lorentzian components were required. The time constant, τ, corresponding to f_c, was calculated from:

$$\tau = \frac{1}{2\pi f_c}. \tag{2}$$

If it is assumed that channels are identical and independent, and open to only one single-channel current level, i, then i can be estimated from:

$$i = \frac{\sigma^2}{I_N(1-p)}, \tag{3}$$

where I_N is the macroscopic current change in response to muscarine application, σ^2 is the variance of the macroscopic current and p is the probability of the channel being open (see Sigworth, 1980). The variance, σ^2, was estimated in two ways: (i) directly from the sampled data, and (ii) from the area under Lorentzian curves fitted to the power spectra. Good agreement between estimates of the single-channel conductance was obtained for the two methods. In some cases the variance of segments of current was calculated using NAQ5.

Using the measured whole-cell M-current (I_N) and variance (σ^2) estimated from spectral analyses, the total number (N) of available 'M-channels' and the probability of being open (p) at a given membrane potential was estimated from the relationship:

$$\sigma^2 = i[I-(I^2/N)], \tag{4}$$

which can be obtained by eliminating p from eqn (3) (Sigworth, 1980). Experimental data were fitted to eqn 4 using GRAPHPAD and values of i and N obtained. Estimates of p at a given membrane potential, E, were obtained from:

$$p = \frac{I(E)}{[N\,i(E)]}, \tag{5}$$

assuming that the single-channel conductance does not rectify with voltage.

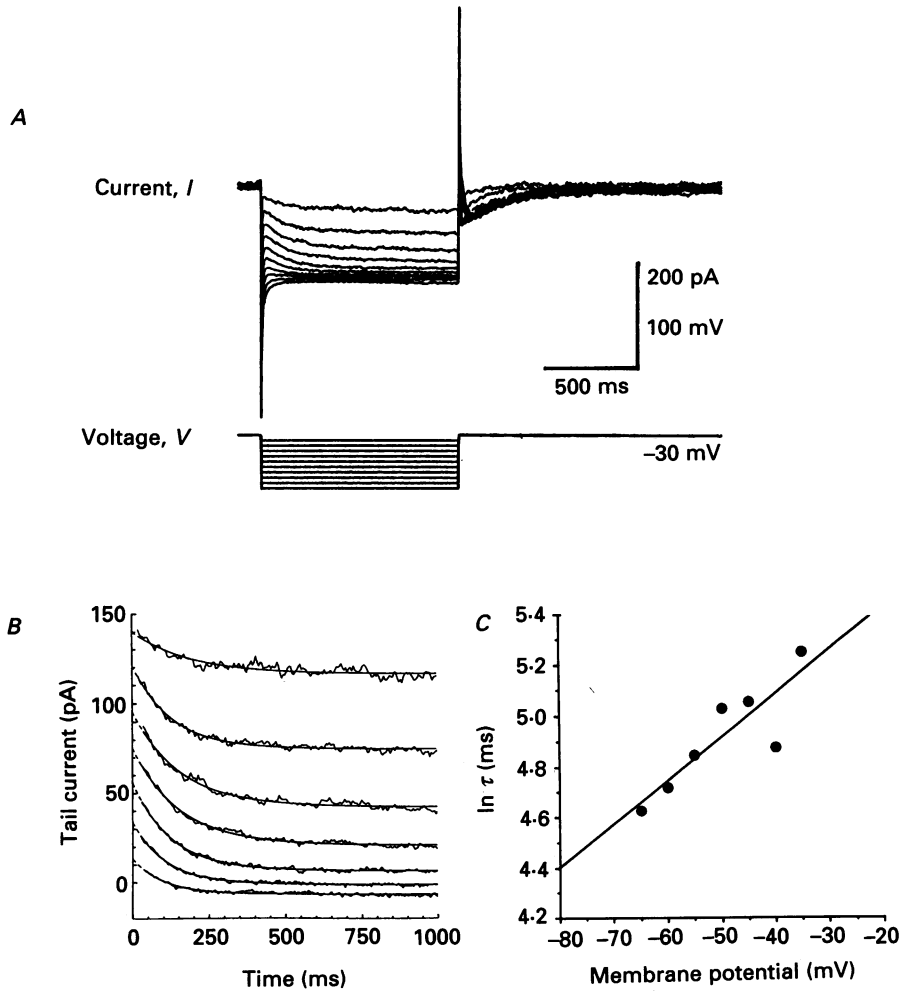

Fig. 1. Voltage-sensitivity of M-current deactivation in whole-cell recording from cultured SCG neurone. *A*, cell is held at −30 mV and the M-current switched off with negative voltage steps of 1 s duration. *B*, deactivation tail currents decay according to a single-exponential function over the whole voltage range, the polarity of tail currents indicating a reversal potential $\geqslant -80$ mV. Recording made in normal recording medium. *C*, the time constant (τ) shortens with hyperpolarization. Plot of ln τ (ordinate) against command potential (abscissa) gives an e-fold reduction in τ for a 60 mV hyperpolarization.

Single-channel conductances were estimated as the chord conductances from i, using:

$$\gamma = \frac{i}{(E - E_{rev})}. \tag{6}$$

RESULTS

M-current relaxations

At −30 mV M-current (I_M) is the dominant outward current in cultured rat SCG neurones (Marrion *et al.* 1987). Hence when the cell is held at this potential and

stepped to more negative potentials, tail currents resulting from the deactivation of I_M can be recorded in almost pure form (Fig. 1*A*). These decayed according to a single-exponential time function over a wide range of potentials (Fig. 1*B*), although in some cells a second, more slowly decaying component was observed (see below).

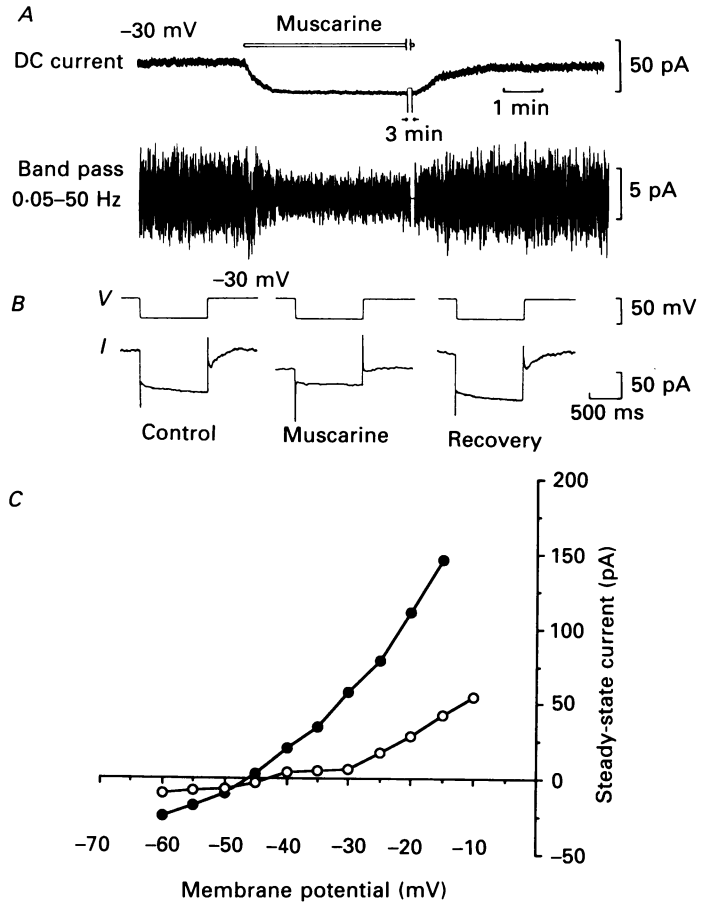

Fig. 2. Muscarine reduces M-current noise. *A*, inward current at −30 mV following application of muscarine (50 μM) by passive diffusion from a micropipette positioned within *ca* 10 μm of the cell body (*upper trace*) and associated reduction in the amplitude of current fluctuations (noise) seen at high gain after AC-coupling the signal (*lower trace*). *B*, reduction in noise is also associated with loss of time-dependent M-current tails following negative voltage steps to −60 mV from the holding potential. *C*, current–voltage (*I–V*) relationships in the presence (○) and absence (●) of muscarine showing cross-over in the *I–V* curves.

As reported previously for these cells (Constanti & Brown, 1981; Brown *et al.* 1989), the time constant for deactivation (τ_{off}) was voltage sensitive, decreasing e-fold for a 60 mV hyperpolarization (Fig. 1*C*). These M-current relaxations are typical of those recorded from over thirty-five neurones. No obvious differences were observed

between recordings in which the recording pipette did or did not contain GTP. The reversal potential for I_M, estimated from the reversal of the deactivation relaxations (e.g. Fig. 1*A*), was normally between −70 and −90 mV.

Muscarine-sensitive currents

Application of muscarine at −30 mV caused a slowly developing reduction in the standing outward current (Fig. 2*A*, top trace). This was associated with the loss of

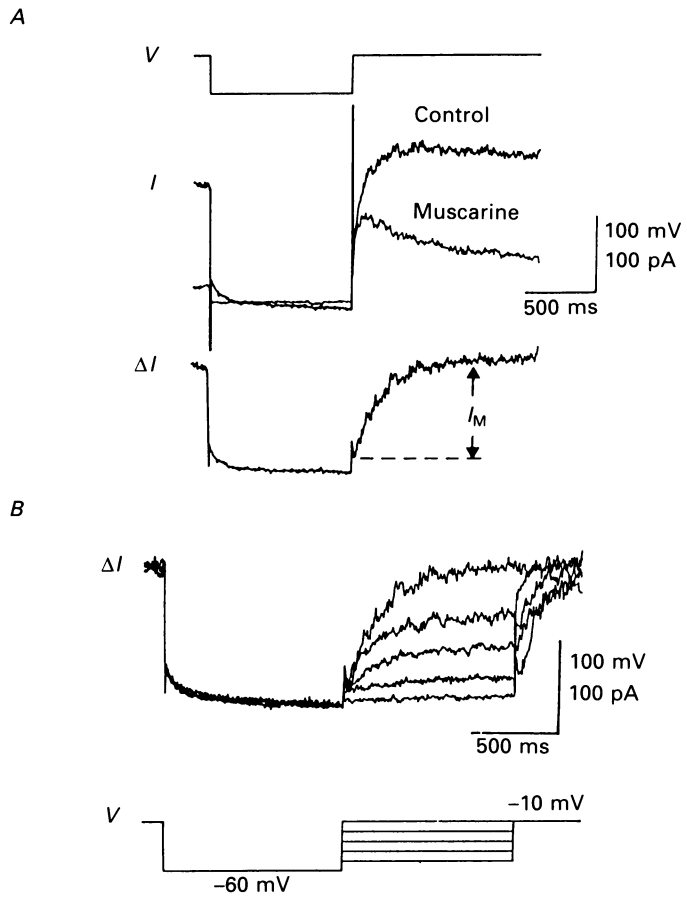

Fig. 3. Isolation of muscarine-sensitive current. *A*, current responses to negative voltage jump from −10 to −60 mV. Middle panel shows two superimposed currents recorded ±muscarine. Lower panel (Δ*I*) shows the result of subtracting the residual current in the presence of muscarine from the control and thus represents the muscarine-sensitive component of the whole-cell current. *B*, whole-cell muscarine-sensitive currents (Δ*I*, obtained by subtraction as in *A* for a series of voltage jumps (superimposed)). Note small instantaneous currents at the beginning of the depolarizing voltage steps.

the time-dependent M-current deactivation and reactivation current relaxations induced by hyperpolarizing steps (Fig. 2*B*) and a reduction of the amplitude of the current fluctuations (noise) recorded at high gain (Fig. 2*A*; lower trace).

Current–voltage (*I–V*) curves in the presence and absence of muscarine were

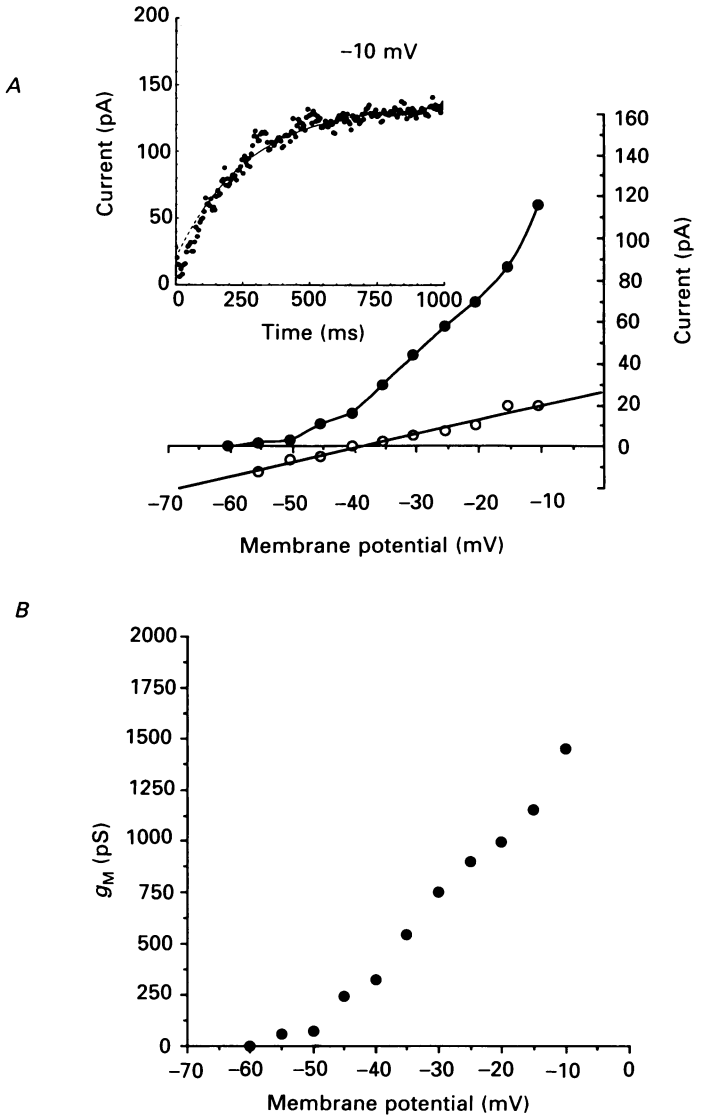

Fig. 4. Two components of muscarine-sensitive current. *A*, steady-state currents calculated from the fitted exponential curves to muscarine-difference currents (see Fig. 3*B*). Inset shows muscarine-sensitive current activated by a voltage step from −60 to −10 mV: the current, excluding the first twenty data points (dashed line), is fitted with a single-exponential function plus a constant (continuous curve). Steady-state values were obtained for the time-dependent current from the exponential fit ($t = \infty$) and the current–voltage curve plotted as filled circles. Instantaneous current was obtained from the fitted off-set values and is plotted as open circles. The instantaneous current–voltage relation is linear and reverses at *ca* −40 mV. Threshold for activation of the time-dependent current (I_M) is *ca* −55 mV. *B*, conductance–voltage relationship for the whole-cell M-current derived from the data in *A* assuming a reversal potential of −90 mV.

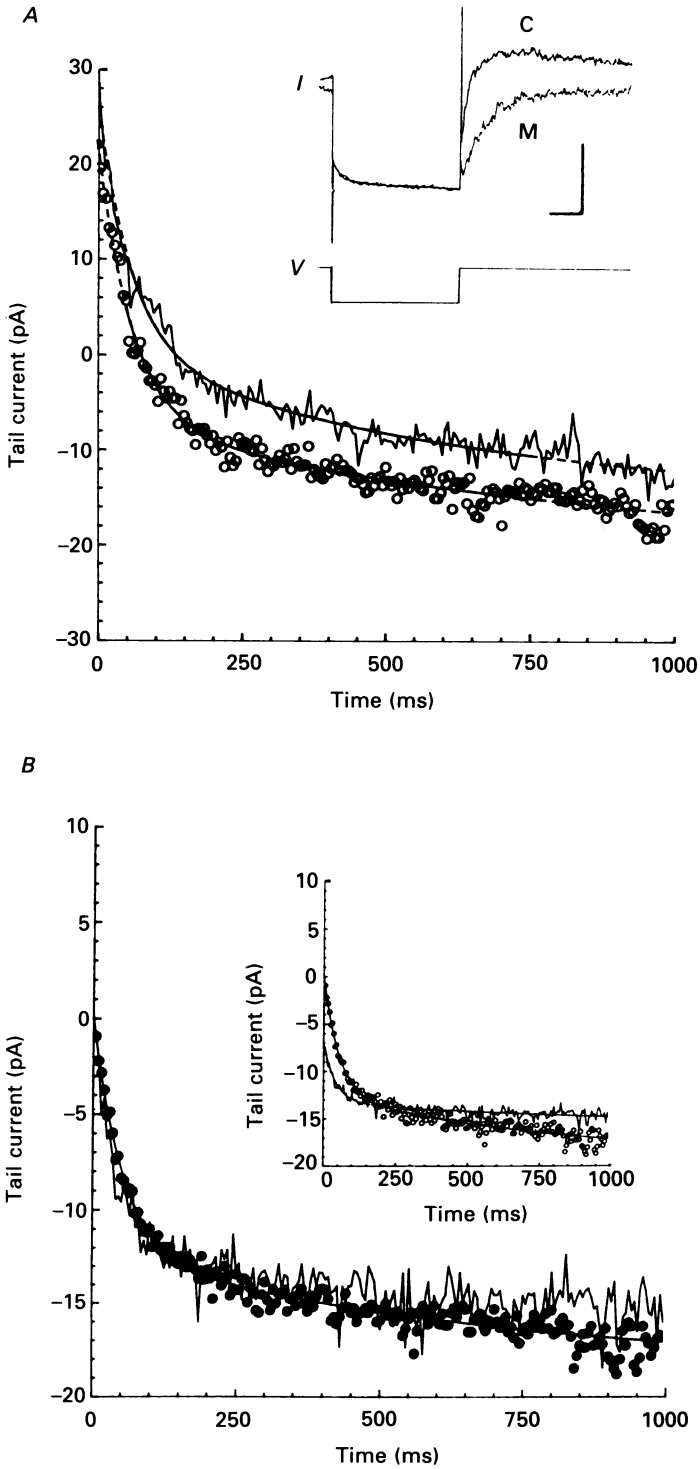

Fig. 5. For legend see facing page.

constructed using a series of hyperpolarizing and depolarizing steps (cf. Fig. 1). In the cell illustrated in Fig. 2, these *I–V* curves crossed over (Fig. 2*C*), rather than converging close to the resting potential as would be expected were the change in steady-state current due solely to M-current suppression (see Adams, Brown & Constanti, 1982*b*). This suggests the presence of an additional component of muscarine-sensitive current at −30 mV with a reversal potential positive to E_K, as previously reported for *in situ* rat SCG neurones by Brown & Selyanko (1985). This component appears to have no time dependence (see below).

The muscarine-sensitive components of membrane current were further analysed by subtraction methods (Fig. 3*A*) and difference currents were obtained over a range of potentials (Fig. 3*B*). The reactivation current relaxations were fitted by single-exponential functions superimposed on a linear component (e.g. Fig. 4*A*, inset). The *I–V* relationships for the muscarine-inhibited components of current derived from this analysis are shown in Fig. 4*A* and are similar to that obtained by measuring the 'instantaneous' and steady-state currents by eye using a cursor. The corresponding conductance–voltage relationship is shown in Fig. 4*B*, assuming a reversal potential of −90 mV which was estimated from tail current analyses.

The exponential time-dependent component is outward throughout the voltage range, with an activation threshold just positive to −60 mV, as expected for an M-current (Adams *et al.* 1982*a*), whereas the time-independent component was linear and reversed at about −40 mV (Fig. 4*A*). The presence of this component accounts for the cross-over of the *I–V* curves in Fig. 2*C*, the sum of the two components being equivalent to the difference in steady-state current before and after muscarine. We assume (in agreement with Brown & Selyanko, 1985) that the apparently 'linear' component of current represents an additional muscarine-sensitive current, distinct from I_M.

Muscarine does not alter kinetics of I_M

Following complete block of I_M, comparison of 'raw' M-currents and difference currents (i.e. muscarine-sensitive currents) recorded at −60 and −30 mV revealed that, in most cases, the M-current accounted for all of the time-dependent current activated over the range −25 to −60 mV. For example, the amplitude and time course of the deactivation tail current recorded following a voltage step from −10 to −60 mV was identical to the corresponding difference current (Fig. 5*A*). When

Fig. 5. Effect of muscarine on M-current kinetics. *A*, raw (○) and muscarine-sensitive (continuous trace) currents recorded at −60 mV (deactivation tails) are fitted with two-component exponential decay function with $\tau_{control}$ of 63 and 880 ms and $\tau_{muscarine}$ of 58 and 598 ms. Inset: control (C) and muscarine-difference (M) currents (*I*) are shown superimposed; voltage step from holding potential of −10 to −60 mV. *B*, comparison of control tail current (●) with the residual tail current (continuous trace) after partial block of I_M with muscarine. The residual current has been scaled by a factor of *ca* 2 in order to superimpose the control (ordinate calibration refers to control current). The control current has been fitted with two-exponential functions (continuous line) with time constants of 54 ± 4 ms and 775 ± 208 ms. Inset: raw currents recorded in the absence (○) and presence of muscarine (continuous trace). Both tail currents are fitted with a two-component exponential function: the control as above and the residual current with time constants of 40 ± 5 ms and 850 ± 85 ms.

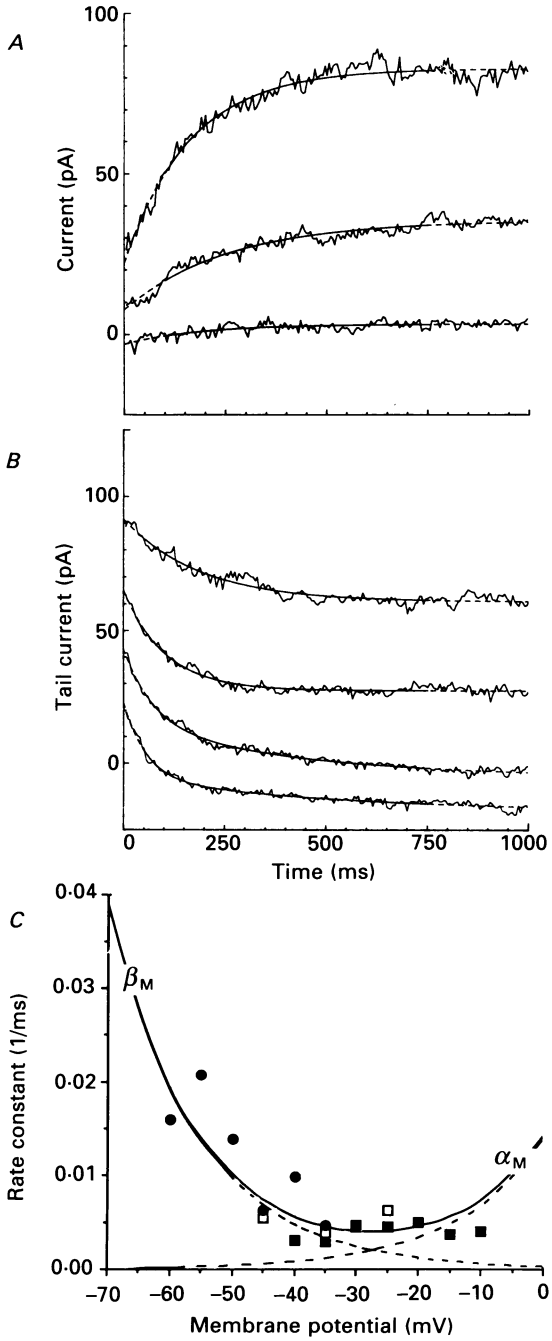

Fig. 6. Voltage sensitivity of M-current relaxations. Raw M-current activation (*A*) and deactivation currents (*B*) recorded from holding potentials of −60 and −10 mV, respectively. Raw M-current activation relaxations are shown at −45, −35 and −25 mV (*A*) and are all fitted with single-exponential functions. Deactivation currents were fitted with single-exponential functions over a range of depolarized potentials in this cell (−30 to −45 mV), whereas tail currents recorded at more negative potentials were best fitted with two-term exponential functions. Deactivation tails illustrated in (*B*) are at −30,

superimposed, the two currents were indistinguishable by eye (Fig. 5*A*, inset). Similarly, the time course and amplitude of raw and difference currents activated by depolarization from −60 to −30 mV were the same ($\tau = 216$ and 220 ms, respectively; not shown).

Deactivation tail currents were also measured during periods of only partial block by muscarine. Under this condition, it was found that the residual current relaxation in the presence of muscarine followed a very similar time course to the raw current which was known from above to be entirely due to I_M (Fig. 5*B*). Thus, the kinetics of M-current deactivation were apparently unaltered by muscarine. The lack of effect of muscarine on the macroscopic kinetics of M-currents suggests that M-channels are shut down in an all-or-none manner. This was an important observation with respect to the subsequent spectral analysis of muscarine-sensitive noise (see below).

Raw activation currents were fitted over only a limited range of membrane potentials (Fig. 6*A*) due to contamination with other voltage-activated outward currents at more depolarized potentials (e.g. Fig. 5*A*, inset). Over this range, time constants obtained for raw and difference currents were similar. Note that, although deactivation tails recorded at potentials more negative than −50 mV were fitted with a two-term exponential function in this cell, at more depolarized potentials (−30 to −50 mV) tails were fitted by a single-exponential function (Fig. 6*B*). In the original description of M-current kinetics (Adams *et al.* 1982*a*), a simple open–closed scheme for the M-channel was assumed with activation controlled by a single voltage-sensing particle, viz.

$$\text{Closed} \underset{\beta_M}{\overset{\alpha_M}{\leftrightarrow}} \text{Open}$$

and where the probability of a channel being in the open state was governed by a Boltzmann distribution. The forward and backward rate constants (α_M and β_M, respectively) may then be expected to vary with voltage according to

$$\alpha_M = \alpha_M(0) \exp[(+ze/2kT)(V - V_0)] \tag{7}$$

and

$$\beta_M = \beta_M(0) \exp[(-ze/2kT)(V - V_0)], \tag{8}$$

(Adams *et al.* 1982*a*), where z is the effective valency of the voltage-sensing particle, k and T have their usual meanings and V_0 is the voltage at which half-maximal activation of I_M occurs. The combination of eqns (7) and (8) will describe the voltage dependence of the time constant, τ_M, which is

$$(\tau_M)^{-1} = \alpha_M + \beta_M. \tag{9}$$

−40, −50 and −60 mV (top to bottom). The voltage sensitivity of rate constants derived from these analyses (the fast component in the case of two-component relaxations) is shown in *C*. Values of rate constants were obtained, in the same cell, from raw deactivation tails (●), raw activation relaxations (□) and activation relaxations of muscarine-difference currents (■). Dashed lines represent the theoretical variation of the opening and closing rate constants of the M-channel (α_M and β_M, respectively), assuming that

$$\alpha_M = \alpha_M(0) \exp[(+ze/2kT)(V - V_0)] \quad \text{and} \quad \beta_M = \beta_M(0) \exp[(-ze/2kT)(V - V_0)],$$

where $z = +3{\cdot}5$, $V_0 = -27{\cdot}5$ mV, $\alpha_M(0) = \beta_M(0) = 0{\cdot}002$/ms (see text). The continuous line represents the voltage sensitivity of the M-current time constant from: $(\tau_M)^{-1} = \alpha_M + \beta_M$.

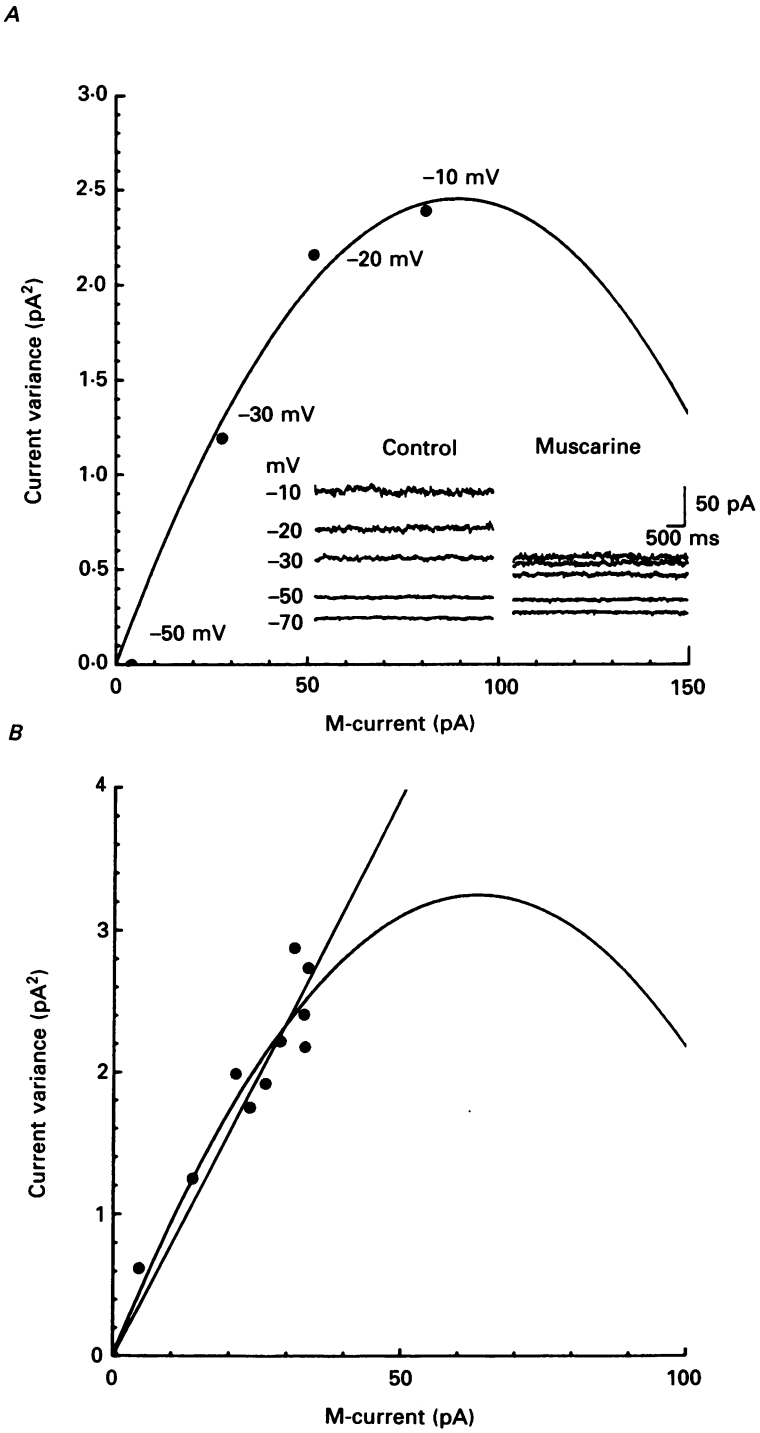

Fig. 7. For legend see facing page.

Figure 6*C* shows how our results compare with the predictions of this model where the dashed lines describe the theoretical voltage sensitivity of α_M and β_M ($z = +3{\cdot}5$, $V_0 = -27{\cdot}5$ mV and $\alpha_M(0) = \beta_M(0) = 0{\cdot}002$/ms) and the continuous curve represents the variation of $(\tau_M)^{-1}$ with voltage. Using this model, the intersection of the reciprocal time constant–voltage curves would indicate that half-maximal activation of I_M occurs at about -28 mV (Fig. 6*C*). Although experimental data obtained at negative potentials support this model, analysis of relaxations recorded at more positive potentials is required to properly evaluate the degree of voltage sensitivity of the forward rate constant (α). In view of the uncertainty in α we have chosen not to derive a half-maximal activation voltage and probability of opening from the fitted curve.

Fluctuation analysis of M-current

As shown in Fig. 2*A*, a clear reduction in the amplitude of current fluctuations ('noise') was seen when muscarine was applied at clamp potentials $\geqslant -40$ mV. The relationship between the variance of this muscarine-sensitive component of current noise and the mean current was determined for a range of membrane potentials. Current variances recorded in the presence and absence of muscarine were subtracted and plotted against mean muscarine-blocked current after normalizing (see legend Fig. 7*A*) both current and variance with reference to a holding potential of -10 mV, assuming a reversal potential of -90 mV (i.e. driving force of 80 mV) (Fig. 7*A*). The data were fitted according to eqn (4), from which i and N were estimated to be 0·06 pA and 3236, respectively. From eqn (5), p was estimated to be *ca* 0·1 at -30 mV.

The relationship between the current and variance associated with recovery from muscarine block at a constant membrane potential (-30 mV) was also examined. It was found that the data were well fitted by a linear regression (Fig. 7*B*). The simplest interpretation of this result is that no measurable change in p has occurred during the unblocking process and that the increase in current simply reflects an increase in the number of channels available. Assuming that this is the case, then the slope of the line is equal to the single-channel amplitude (i) at this potential (-30 mV) which, in this example, was estimated to be 0·08 pA (chord conductance, 1·3 pS). We cannot, however, exclude the possibility that p is reduced in the presence of muscarine which

---

Fig. 7. Current–variance relationships for M-current. *A*, plot of variance of the muscarine-sensitive macroscopic current (σ^2) and mean muscarine-sensitive current (I_N) measured at various membrane potentials (inset: raw data obtained at indicated membrane potentials ± muscarine). Current and variance have been normalized to a constant driving force in each case according to:

$$I = I(V)[(-10 - V_{eq})/(V - V_{eq})] \quad \text{and} \quad \sigma^2 = \sigma^2(V)[(-10 - V_{eq})^2/(V - V_{eq})^2].$$

The data have been fitted with a parabola of the form $\sigma^2 = I/(iN)$, where $i = 0{\cdot}06$ pA and $N = 3236$. At -30 mV p is *ca* 0·1. *B*, plot of muscarine-sensitive current and current variance, obtained during the recovery from block by muscarine, of outward current recorded at -30 mV (raw data shown in Fig. 2*A*). Variance (σ^2) and current (I) were calculated over successive 20 s periods during recovery. Data have been fitted with a linear regression (slope = 0·08 pA, $r = 0{\cdot}961$) and a parabolic function of the form described in *A* ($i = 0{\cdot}1$ pA, $N = 1238$, $p = 0{\cdot}2$, $r = 0{\cdot}964$); see Discussion.

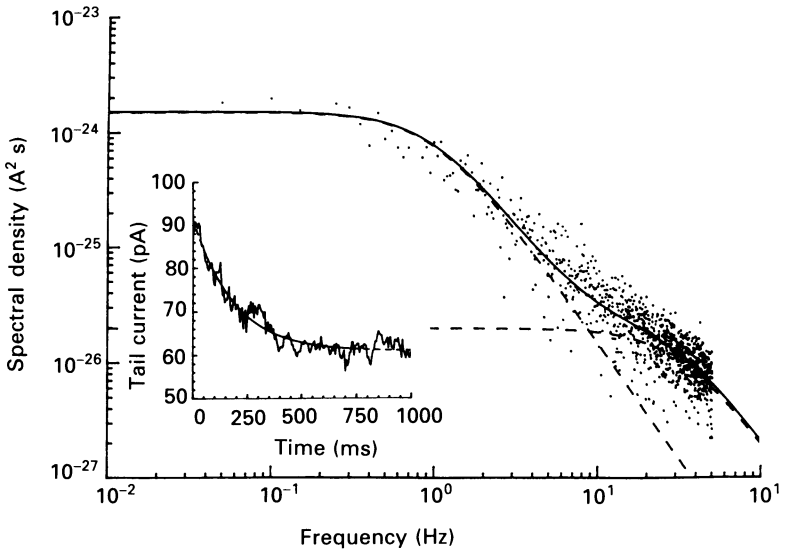

Fig. 8. Spectral density plot of M-current noise. Net spectrum obtained by subtraction of the average of spectra in the presence (average of 22) and absence (average of 17) of 50 μM-muscarine (see Methods). Contiguous segments of current were recorded at a holding potential of -30 mV (same cell as in Fig. 7) for a period of several minutes under each condition. Current was filtered between 0·05 and 50 Hz; sampling rate 100 Hz. The power spectrum is fitted with a two-component Lorentzian function where $G(0)_1 = 1{\cdot}50$ pA^2 s $G(0)_2 = 0{\cdot}02$ pA^2 s, $f_{c1} = 0{\cdot}98$ Hz, $f_{c2} = 32{\cdot}90$ Hz. Inset shows a whole-cell M-current deactivation tail current recorded at -30 mV in the same cell. The relaxation is fitted with a single-exponential function having a time constant of decay of 187 ms. The total variance accounted for by the two Lorentzian components is 3·32 pA^2.

TABLE 1. Pooled values of time constants and elementary conductance (γ) from five separate estimations (each estimation obtained from the fitting of a net spectrum derived from an average of fourteen to twenty-two individual raw spectra). All spectra obtained at a clamp potential of -30 mV.

	Mean ($n = 5$)	S.E.M.
τ_1	162 ms	4·7
τ_2	15 ms	3·1
γ	1·0 pS	0·2

would give rise to the parabolic relationship between variance and current (I) indicated in Fig. 7*B* (see Discussion).

Spectral analysis

The spectral density function for the muscarine-sensitive current in the same cell was obtained as described in the Methods, and is illustrated in Fig. 8. The observed spectrum has been fitted with two Lorentzian components.

The characteristic corner frequencies, f_{c1} and f_{c2}, were 0·98 and 32·9 Hz, respectively, which would correspond to time constants of 162 and 5 ms, respectively. The putative single-channel amplitude was calculated from the ratio of the variance (obtained from the fitted spectrum where $\sigma^2 = (\pi/2)(\Sigma G(0) f_c)$ to the macroscopic current blocked by muscarine. If it is assumed that a single species of channel, that opens to only one conductance level, accounts for the total variance and that the

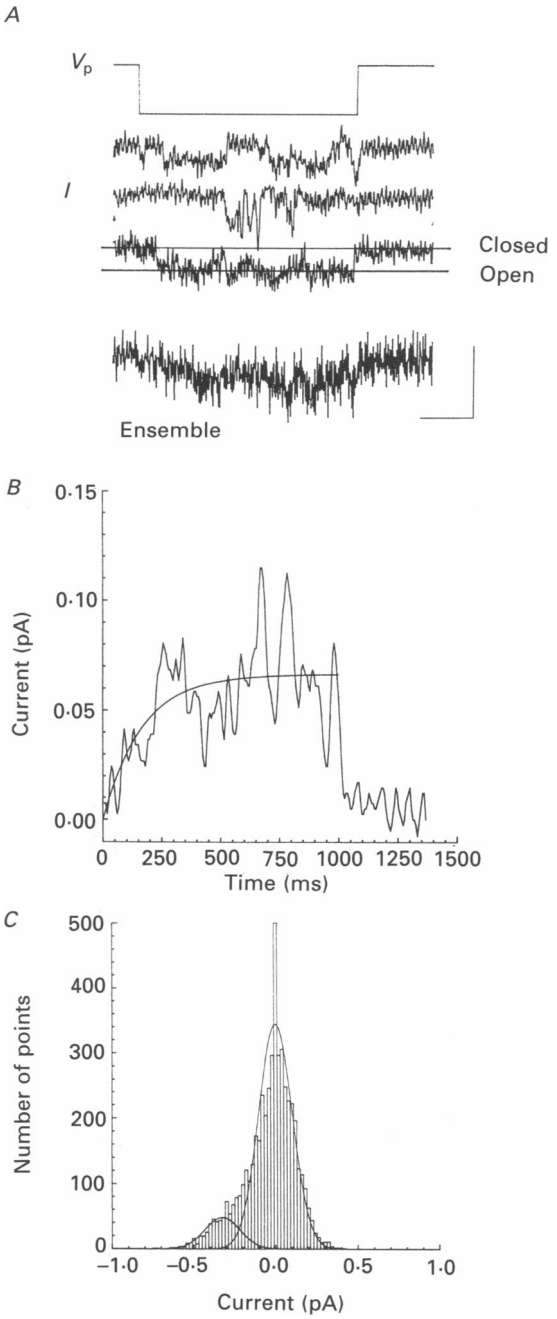

Fig. 9. Low-amplitude, single K^+ channels in cell-attached patches. *A*, selected records recorded in a cell-attached patch configuration with a pipette containing isotonic KCl (180 mM) and 1 μM-apamin. The patch was held at 10 mV depolarized to rest (i.e. pipette potential, $V_p = -10$ mV) and depolarizing voltage jumps made at 0·1 Hz to +80 mV relative to rest (i.e. $V_p = -80$ mV; cell resting membrane potential assumed to be *ca* −60 mV). Single-channel records have been leak subtracted. Bottom trace: ensemble average of twenty-two such records, containing channel openings (downwards represents open ≡ outward current) from a total of forty-seven jumps (twenty-five null jumps). Note

linear component of the muscarine-sensitive current (see above) does not contribute to the variance measured over this bandwidth, then the single-channel conductance is estimated to be 1·7 pS. If it is assumed that the linear component of muscarine-sensitive current (above) contributes the observed higher frequency component of the power spectrum (which is, however, unlikely since its apparent reversal potential is close to −30 mV) and that I_M gives rise to the lower frequency component only (Fig. 8), then the single-channel conductance calculated from this low frequency component is 1·2 pS. The time constant of the raw M-current deactivation tail at this potential was found to be 187 ms (Fig. 8, inset), in close agreement with the time constant of the low frequency component. The mean value of τ_1 (from five cells) was 162 ms (Table 1).

Single-channel recording

Single-channel recordings were made using both cell-attached and outside-out configurations (Hamill *et al.* 1981). Although small-amplitude channels were observed in many patches, these were usually too small to resolve. However, in a few this was made possible by filtering strongly (100 Hz). An example of current records obtained from a cell-attached patch is shown in Fig. 9*A*. The recording pipette contained an elevated $[K^+]$ (180 mM) in order to amplify the K^+ currents and also to provide symmetrical recording conditions (assuming an intracellular $[K^+]$ of *ca* 180 mM: see Marrion, 1988). The channel was apparently activated following depolarizing voltage steps from the nominal resting potential of the cell (Fig. 9*A*). An ensemble average of several such records exhibiting openings resembled whole-cell M-current relaxations with respect to the time dependence of the process (Fig. 9*A*). The relaxation was fitted with a single-exponential function having a time constant of 164 ms (Fig. 9*B*).

The probability of being open (p_{open}), calculated from the ensemble as the proportion of the mean open-channel amplitude was remarkably low (0·006, taking into account null jumps). Individual openings often appeared to be long lasting (hundreds of milliseconds), although the filter settings required for these experiments would have obscured brief transitions to the closed state.

A histogram of individual data points from the same current records which gave rise to the ensemble shown in Fig. 9*C*, indicates a mean single-channel amplitude of 0·4 pA at the estimated membrane potential of +20 mV (Fig. 9*C*). The transmembrane potential was estimated assuming a resting membrane potential of −60 mV (typical) and the apparent reversal potential of single outward channels (E_K *ca* 0 mV actual membrane potential). The single-channel conductance was thus estimated to be 21·5 pS. If it is assumed that the channel obeys the constant-field

---

that the downward-going relaxation represents *outward* current in this recording configuration. *B*, the ensemble average (inverted and smoothed) follows a single-exponential function (data is shown from the start of the voltage jump only) having a time constant of 164 ms. *C*, amplitude histogram of all data points from records exhibiting openings as in *A*. The large peak which is normally distributed about a mean of *ca* 0 pA represents baseline points or the 'closed state'. The smaller peak which represents open channels is also normally distributed (mean = 0·4 pA). Calibration: 100 mV, 1·0 pA, 0·2 pA (ensemble), 250 ms. Currents filtered at 100 Hz.

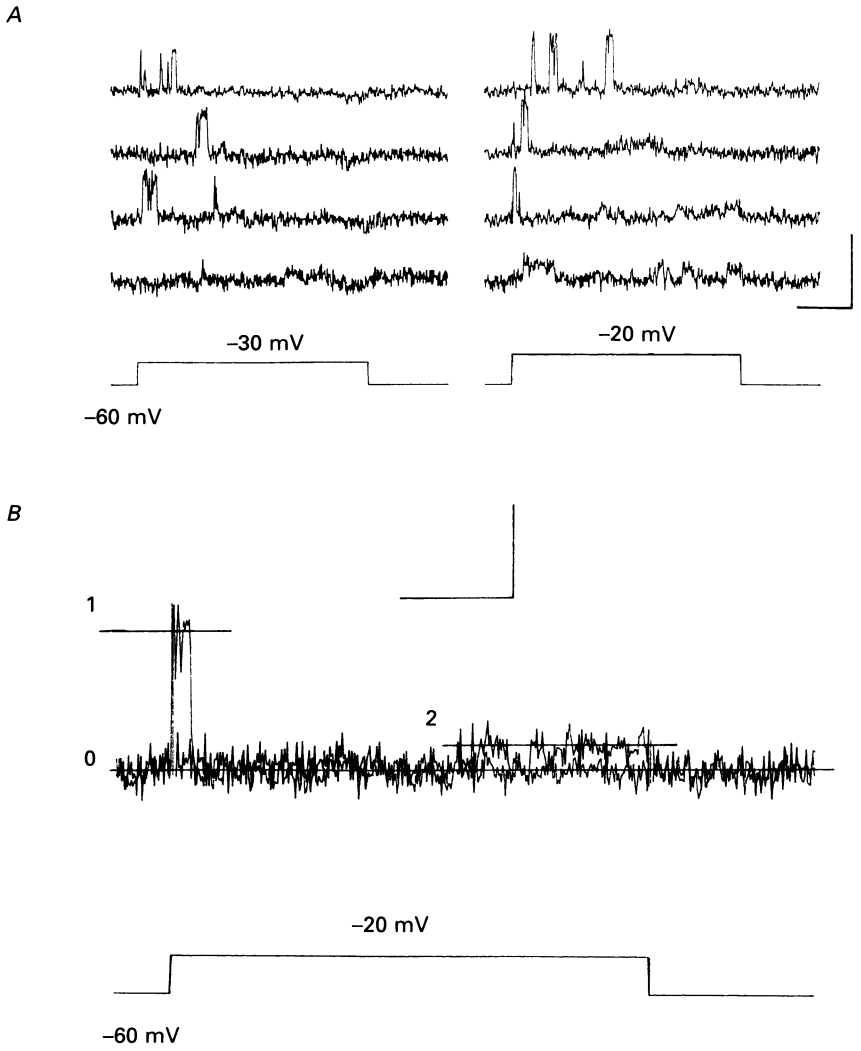

Fig. 10. Low-amplitude channels in outside-out membrane patches. *A*, representative records recorded in the outside-out patch clamp configuration using normal intracellular and extracellular recording solutions. Outward single channels activated by depolarizing voltage steps, from the holding potential of −60, to −30 mV (left) and −20 mV (right). The current records have been leak-subtracted. *B*, the channels fall into two groups: a larger amplitude channel (1) which tended to cluster around the beginning of the voltage step, and a smaller channel of relatively long duration (2) which occurred throughout the depolarization, although in this example it occurred at the end of the 1 s long step (closed state: 0). The mean current amplitudes of the large and small channel (measured by hand) were 0·8 pA (11·5 pS) and 0·2 pA (2·6 pS), respectively. Calibrations: *A*, 1·0 pA, 100 mV, 250 ms; *B*, 0·5 pA, 100 mV, 250 ms. Currents filtered at 100 Hz.

equation (Goldman, 1943; Hodgkin & Katz, 1949) then the predicted conductance of this channel in physiological [K^+] (at -30 mV) would be about 4 pS. Small-amplitude channels approximating this size were detected in about six out of twenty-eight cell-attached patches.

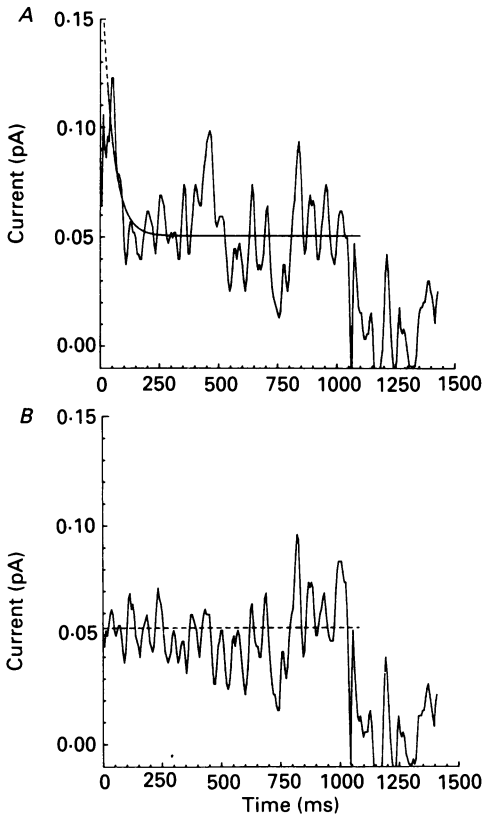

Fig. 11. Time dependence of low-amplitude channel in outside-out patches. Ensemble averages obtained from currents obtained from voltage jumps from -60 to -20 mV (0·1 Hz; same patch as in Fig. 10). *A*, ensemble average (thirty-three out of fifty-nine jumps in total) of current records containing both large- (A-type channel) and small-amplitude channel. Relaxation is fitted with a single-exponential function ($\tau = 44$ ms) superimposed upon a constant offset value. *B*, ensemble average obtained for records including only the small-amplitude channel (thirty-three out of fifty-nine jumps). The larger channel ('A' channel) was excluded by a post-acquisition editing process (see Methods). This ensemble shows no time dependence. Data are shown from the start of the voltage step (-60 to -20 mV for 1 s) only.

Attempts to turn off the channel by applying muscarine to the cell membrane outside the patch were unsuccessful in this and other cell-attached patches. Conclusive results were hampered by a tendency for the small channel to turn off for protracted periods of time and in some cases suspected changes in the cell's membrane potential upon muscarine application (action potentials were occasionally triggered and reflected in the patch).

A small-amplitude channel was also identified in outside-out patches, although often together with a larger, more easily resolved channel (Fig. 10*A*). The small-amplitude channel was detected in about five out of twelve outside-out patches and the larger ('A' type, see below) somewhat more frequently. The larger channel (*ca* 11·5 pS) tended to cluster near the beginning of depolarizing voltage steps whereas the small-amplitude channel (*ca* 2·6 pS) showed little time dependence over a number of jumps. This was illustrated by ensemble averages of the records in which the larger channel was both included and excluded (by editing, see Methods). The ensemble average obtained for the small-amplitude channel alone shows no time dependence (Fig. 11*B*), whereas with all channels included a pronounced early transient component can be seen (Fig. 11*A*). The time constant of decay of this transient component ($\tau = 44$ ms) is similar to the time constant of inactivation of the whole-cell transient outward current (I_A) recorded in SCG neurones under similar conditions (not shown). The probability of the small channel being open (p) was estimated from the amplitude of the ensemble average current of all jumps, including null jumps, to be 0·002.

Although channels of similar amplitude were observed in other outside-out patches, often these patches contained other types of channel (probably K^+ channels) as well. In particular, a channel of 6–8 pS, characterized by its rapid and continuous activity over a wide range of potentials, was commonly seen. This effectively obscured any other channel activity of smaller conductance and appeared to be a phenomenon associated with the outside-out configuration particularly. These factors presented difficulties in adequately testing whether or not the smaller amplitude channel was sensitive to muscarine when applied to the external membrane. Furthermore, as in cell-attached patches, the small-amplitude channel would periodically enter a refractory state, which rendered equivocal the results of the few attempts at block.

DISCUSSION

Using the patch clamp technique we have observed very clear reductions in the amplitude of membrane current noise during application of muscarine. We believe this results from closure of M-channels since it is correlated with inhibition of the M-current deactivation relaxations recorded simultaneously, and the longer time constant derived from spectral analysis of the noise reduction agreed with the time constant for the M-current relaxation at the same voltage (see below). We have accordingly tried to deduce some of the elementary properties of the M-channels by analysis of the noise reduction induced by muscarine, i.e. by subtracting the residual noise in the presence of muscarine from that in its absence. This is based on the assumption that muscarine itself does not affect the time constants of the spectrum or the relative amplitude of its components but simply closes a proportion of M-channels. The evidence for this is that the time course of the macroscopic current relaxation recorded in the absence of muscarine (at potentials where there were no other contaminating time-dependent currents) was the same as that of residual M-current recorded in the presence of muscarine. Furthermore, difference spectra were obtained under conditions of complete block of I_M by muscarine.

Subtracted power spectra of the (muscarine-sensitive) current noise could be fitted

by two Lorentzian functions, with corner frequencies corresponding to time constants of 5 and 162 ms. One possible interpretation of this is that two distinct types of channel contributed to the muscarine-inhibited current noise. Macroscopic current measurements did indeed frequently reveal two components of inward current induced by muscarine – a time-dependent component corresponding to the M-current, with a time constant corresponding to the longer time constant of the Lorentzian spectra, and an apparently time-independent component (under the recording conditions) reversing at about −40 mV. This latter component might correspond to the shorter component of the Lorentzian since any relaxations yielded by such fast channel closure would appear as an 'instantaneous' component of current during a voltage step at the data sampling rate used in our experiments. However, there are two arguments against this latter hypothesis. Firstly, the linear component of muscarine-sensitive current was not apparent in all whole-cell recordings, whereas (at membrane potentials of −30 mV, at least) observed power spectra always required two Lorentzians. Secondly, since the linear component reversed at −40 mV, it would contribute little variance at −30 mV. We therefore suggest that both components reflect the activity of a single channel type, but capable of adopting three kinetically distinguishable states. For example, the longer time constant might then reflect the mean duration of bursts of openings. In single-channel patches (see below) some channel openings appeared to last hundreds of milliseconds. However, since it was necessary to filter the records heavily (100 Hz) to discriminate these channels from patch noise, these recordings have not, so far, been helpful in this regard.

The parabolic relationship between current and variance obtained over a range of membrane potentials, suggested that at −30 mV the probability of the M-channel being open (p) was *ca* 0·1. Although p was apparently not $\ll 1$, and therefore the single-channel amplitude was not directly equal to the ratio of variance to current (see Neher & Stevens, 1977), our estimate of the single-channel conductance (on the basis of this estimate of p) is nevertheless unlikely to be underestimated by more than about 9%. With this proviso, our estimate of the elementary conductance of the M-channel (from noise analysis) at −30 mV is about 1–2 pS.

The apparently linear relationship between the magnitudes of current and variance during the unblocking of I_M is consistent with an all-or-none type of block with no change in the probability of 'active' M-channels being open (p), as has been described for the block by serotonin of S-channels in *Aplysia* sensory neurones (Belardetti, Kandel & Siegelbaum, 1987). In fact, the current–variance data are equally well fitted by a parabola relating current and variance to the parameters i and N (see Fig. 7*B*) and we cannot, therefore, exclude the possibility that muscarine may reduce p for 'active' channels. The best-fit parabola to this data estimates the single-channel amplitude to be 0·1 pA and N to be 1238. Taking these values, p was estimated to be *ca* 0·2 and thus, from $p = 1/(1+\beta/\alpha)$, $\beta/\alpha = 4$. If this were the correct interpretation of the data, the time constant estimated from the spectral analysis may be underestimated by about 20%. Similarly, the elementary current amplitude may be underestimated by *ca* 20%. The lack of effect of a 50% blocking concentration of muscarine on the time constant of deactivation at −65 mV suggests that muscarine is unlikely to effect the closing rate of the M-channel at least. More

information will be required regarding the [muscarine] dependence of M-current block and amplitudes of the estimated elementary parameters in order to distinguish between these two models of muscarinic block of M-channels. Meanwhile, although the interpretation of the present data does influence the estimations of the amplitudes of the estimated elementary parameters i and τ the subtraction procedure used to obtain spectral density distributions remains valid since the data in these cases were obtained under conditions of complete block of I_M.

From the amplitude of the maximum M-current at strongly depolarized levels (Fig. 4), we might expect to be able to activate *ca* 1000–1500 M-channels in the typical cultured SCG neurone. In fact, our estimate of the total number of M-channels *available* for opening (N), obtained from current–variance data is roughly in accordance, ranging between about 1200 and 3200.

In cell-attached patches, one type of channel which might be the elementary M-channel could be detected following heavy filtering. This channel showed long open times and the envelope current generated by repeated depolarizing commands showed a time constant for channel opening similar to that for the macroscopic current recorded under whole-cell clamp. The single-channel conductance recorded at +20 mV in isotonic K^+ was 21·5 pS, which translates to about 4 pS at −30 mV in 2·5 mM-K^+, assuming constant-field rectification. Although somewhat higher than that predicted from the noise analysis, a similar discrepancy between recorded single-channel conductance and the apparent elementary conductance yielded by noise analysis has been noted for other low-conductance channels (e.g. Marty, Tan & Trautman, 1984; Capiod & Ogden, 1985, 1989).

It is clear that M-channel closure induced by muscarine requires activation of a GTP-binding protein (Pfaffinger, 1988; Marrion *et al.* 1989; Lopez & Adams, 1989) but it is still unclear whether subsequent steps involve a soluble cytoplasmic messenger. One good reason for studying single M-channels is to resolve this question. Unfortunately, we have not yet been able to do so. Thus, in a limited number of tests we have so far not detected a clear inhibition of the low-conductance channel recorded in cell-attached patches on applying muscarine outside the patch (as might be expected for a cytoplasmic messenger) but these experiments have been hampered by the low probability of in-patch channel opening with repeated voltage jumps, coupled with the tendency of the channels to enter long silent periods. On the other hand, for the same reasons, we have been unable to test adequately a more local effect of muscarine on the equivalent low-conductance channels seen in outside-out patches; as a result, since the opening of these channels did not show clear time dependence, we have no other way of determining whether they are kinetically modified M-channels or some other low-conductance channel. Thus, although an important first step has been made in the identification and characterization of the M-channel in neurones, resolution of the messenger question and mechanism of M-channel block must await further experiments.

We thank Professor D. Colquhoun for the use of noise analysis programs and helpful comments on the manuscript. We also thank J. Dempster for the gift of the noise analysis program NAQ5. This work was supported by a grant from the Medical Research Council.

REFERENCES

ADAMS, P. R., BROWN, D. A. & CONSTANTI, A. (1982*a*). M-currents and other potassium currents in bullfrog sympathetic neurones. *Journal of Physiology* **330**, 537–562.

ADAMS, P. R., BROWN, D. A. & CONSTANTI, A. (1982*b*). Pharmacological inhibition of the M-current. *Journal of Physiology* **332**, 223–262.

BELARDETTI, F., KANDEL, E. R. & SIEGELBAUM, S. A. (1987). Neuronal inhibition by the peptide FMRFamide involves opening of S K^+ channels. *Nature* **325**, 153–156.

BROWN, D. A. & ADAMS, P. R. (1980). Muscarinic suppression of a novel voltage-sensitive K^+ current in a vertebrate neurone. *Nature* **283**, 673–676.

BROWN, D. A., MARRION, N. V. & SMART, T. G. (1989). On the transduction mechanism for muscarinic-induced inhibition of M-current in cultured rat sympathetic neurones. *Journal of Physiology* **413**, 469–488.

BROWN, D. A. & SELYANKO, A. A. (1985). Two components of muscarinic-sensitive membrane current in rat sympathetic neurones. *Journal of Physiology* **358**, 335–364.

CAPIOD, T. & OGDEN, D. C. (1985). Noise analysis of α-adrenergic activated K-conductance in isolated guinea-pig hepatocytes. *Journal of Physiology* **369**, 107*P*.

CAPIOD, T. & OGDEN, D. C. (1989). The properties of calcium-activated potassium ion channels in guinea-pig isolated hepatocytes. *Journal of Physiology* **409**, 285–295.

COLQUHOUN, D., DREYER, F. & SHERIDAN, R. (1979). The actions of tubocurarine at the frog neuromuscular junction. *Journal of Physiology* **293**, 247–284.

CONSTANTI, A. & BROWN, D. A. (1981). M-Currents in voltage-clamped mammalian sympathetic neurones. *Neuroscience Letters* **24**, 289–294.

GOLDMAN, D. E. (1943). Potential, impedance and rectification in membranes. *Journal of General Physiology* **27**, 37–60.

GRUNER, W., MARRION, N. V. & ADAMS, P. R. (1989). Three kinetic components to M-currents in bullfrog sympathetic neurons. *Society for Neuroscience Abstracts* **15**, 990.

HAMILL, O. P., MARTY, A., NEHER, E., SAKMANN, B. & SIGWORTH, F. J. (1981). Improved patch-clamp techniques for high-resolution current recording from cells and cell-free membrane patches. *Pflügers Archiv* **391**, 85–100.

HODGKIN, A. L. & KATZ, B. (1949). The effect of sodium ions on the electrical activity of the giant axon of the squid. *Journal of Physiology* **108**, 37–77.

LANCASTER, B. & PENNEFATHER, P. S. (1987). Potassium currents evoked by brief depolarizations in bullfrog sympathetic ganglion cells. *Journal of Physiology* **387**, 519–548.

LOPEZ, H. & ADAMS, P. R. (1989). A G-protein mediates the inhibition of the voltage-dependent potassium M current by muscarine, LHRH, substance P and UTP in bullfrog sympathetic neurons. *European Journal of Neuroscience* **1**, 529–542.

MARQUARDT, D. W. (1963). An algorithm for least-squares estimation of nonlinear parameters. *Journal of the Society for Industrial and Applied Mathematics* **11**, 431–441.

MARRION, N. V. (1988). Pharmacological control of M-currents in rat sympathetic neurones from the extracellular and intracellular milieux. Ph.D. Thesis, University of London.

MARRION, N. V., SMART, T. G. & BROWN, D. A. (1987). Membrane currents in adult superior cervical ganglia in dissociated tissue culture. *Neuroscience Letters* **77**, 55–60.

MARSH, S. J. & OWEN, D. G. (1988). Fluctuation analysis of M-current in cultured rat sympathetic neurones. *Journal of Physiology* **410**, 31*P*.

MARTY, A., TAN, Y. P. & TRAUTMANN, A. (1984). Three types of calcium-dependent channel in rat lacrimal glands. *Journal of Physiology* **357**, 293–325.

NEHER, E., MARTY, A., FUKUDA, K., KUBO, T. & NUMA, S. (1988). Intracellular calcium release mediated by two muscarinic receptor subtypes. *FEBS Letters* **240**, 88–94.

NEHER, E. & STEVENS, C. F. (1977). Conductance fluctuations and ionic pores in membranes. *Annual Reviews of Biophysics and Bioengineering* **6**, 345–381.

PFAFFINGER, P. J. (1988). Muscarine and t-LHRH suppress M-current by activating an IAP-insensitive G-protein. *Journal of Neuroscience* **8**, 3343–3353.

SIGWORTH, F. J. (1980). The variance of sodium current fluctuation at the node of Ranvier. *Journal of Physiology* **307**, 97–129.